A Combined Calibration of 2D and 3D Sensors
A Novel Calibration for Laser Triangulation Sensors based on Point Correspondences

Alexander Walch and Christian Eitzinger
Machine Vision Department, Profactor GmbH, Steyr-Gleink, Austria

Keywords: Laser Triangulation Sensor, Calibration of Laser Stripe Profiler, Colored Point Cloud, Camera Calibration.

Abstract: In this paper we describe a 2D/3D vision sensor, which consists of a laser triangulation sensor and matrix colour camera. The outcome of this sensor is the fusion of the 3D data delivered from the laser triangulation sensor and the colour information of the matrix camera in the form of a coloured point cloud. For this reason a novel calibration method for the laser triangulation sensor was developed, which makes it possible to use one common calibration object for both cameras and provides their relative spatial position. A sensor system with a SICK Ranger E55 profile scanner and a DALSA Genie color camera was set up to test the calibration in terms of the quality of the match between the color information and the 3D point cloud.

1 INTRODUCTION

Laser triangulation sensors are a widespread instrument to gain 3D information in machine vision applications. They consist of a matrix camera and a laser stripe projector.

The matrix camera is directed onto the plane defined by the laser and is parameterized in a way that only data from points intersecting with this laser plane are captured.

To gain more 3D information than only one profile, laser triangulation sensors are often used to scan objects moved by a conveyor belt or they are mounted on a linear axis.

However, for many inspection tasks it is necessary to obtain information about their textures, in addition to the 3D shape of the objects.

On the one hand such a system is presented in (Munaro et al., 2011), where a colour camera is used for both tasks and additionally two lasers were used to reduce occlusion. For that reason one area in the middle of the image sensor of the camera was used to obtain colour information and the surrounding areas of the sensor serve as laser triangulation sensor, together with the two lasers.

On the other hand there already exist different methods to calibrate pure laser triangulation sensors. Some of them, such as the calibration method provided by the manufacturer of the Ranger E55, only describe a mapping between the image plane and the laser plane of triangulation sensor. This methods lack of information about the spatial position of the sensor. In case of a linear motion of the sensor, it requires to mount the laser in an orthogonal position to the direction of motion. In (McIvor, 2002) a calibration is presented, which uses a 3D calibration object and the used mathematical model fully describes the laser triangulation sensor including its extrinsic parameters.

In this paper we describe in section 2.3 a calibration which only uses data received from the laser plane and does not use the laser triangulation sensors camera as a matrix camera as in (Munaro et al., 2011) and (Bolles et al., 1981). Hence it is also applicable in camera setups which use bandpass filters to block out the surrounding light.

All necessary data for the calibration are obtained from one single scan of the calibration object. This makes the calibration process more efficient, especially because additionally to the laser triangulation sensor, we also calibrate the second camera, which provides colour images.

On the contrary to the algorithm, which is described in (McIvor, 2002) the distance the objects are moved between two captured profiles does not need to be known, but is a parameter of the calibration, which is determined.

Furthermore the novel calibration is easy to implement because either the direct-linear-transformation-algorithm (Abdel-Aziz and Karara, 1971) is used to determine the camera parameters or closed form solu-

Walch A. and Eitzinger C..
A Combined Calibration of 2D and 3D Sensors - A Novel Calibration for Laser Triangulation Sensors based on Point Correspondences.
DOI: 10.5220/0004682900890095
In *Proceedings of the 9th International Conference on Computer Vision Theory and Applications* (VISAPP-2014), pages 89-95
ISBN: 978-989-758-003-1

tions of the arising non-linear optimization problems are presented in this paper.

Since the calibration object of the laser triangulation sensor is also suitable for the calibration of matrix cameras (as described in section 2.4), customized sensor systems can be built, which combine the high 3D data aquisition rate of specialised profile scanner cameras like the SICK Ranger with additional texture information.

In section 3 a setup of the 2D/3D sensor is presented, which was used to perform experiments and to evaluate the calibration. Additionally results of experiments, which were performed with a simulated laser triangulation sensor, are visualised.

Finally in section 4 we discuss the results of the experiments and make some proposals for improvements and future work.

2 CALIBRATION OF THE 2D/3D VISION SENSOR

2.1 The Calibration Object

The calibration object delivers the needed information to determine the parameters of the mathematical models of the cameras. For this reason it contains points with well known coordinates in an arbitrary, predefined coordinate system. An necessary property of these corners is that they can be found in the raw data of the cameras.

The object, which is used to calibrate the 2D/3D sensor, consists of 2 nonparallel planes with checkerboard patterns (3D calibration object). Its advantage is that finding its points, the inner corners of the checkerboards , is a well researched problem and there already exist algorithms, which provide their pixel coordinates on the image of the color camera and also in the raw data provided from the SICK Ranger seen on figure 1.

For the calibration of the matrix camera the row and column coordinates of the found corners on the colour image are used, but a scan of the calibration object of the laser triangulation sensor contains more information. The pixel coordinates $c = \left(c_x, \quad c_y, \quad c_z\right)^\mathsf{T}$ of a corner are 3-dimensional, because the laser triangulation sensor yields its raw data in form of a range image on which every row corresponds to one profile of the scanned object.

- c_x: The x-coordinate of a corner on the range image of the profile scanner (corresponding to the x-coordinate on the image plane of the matrix camera).

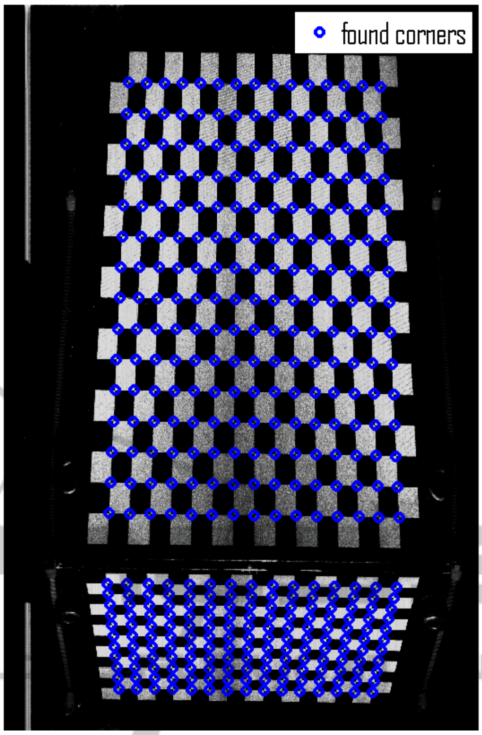

Figure 1: In addition to the range images, laser triangulation sensors often provide intensity images, which do not contain 3D information, but the intensity of the reflected laser light. This images can be used to find the c_x and c_y coordinate of the corners.

- c_y: The y-coordinate of a corner on the range image, corresponding to the number of scanned profiles until the particular corner intersected the laser plane.
- c_z: The range value, which represents the height of the corner and corresponds to the y-coordinate on the image plane.

Since the same points are used for the calibration of both cameras, both mathematical models are located in the same coordinate system and it's therefore easy to combine the colour information with the 3D point cloud.

2.2 Correcting the Lens Distortion

The lens distortion of the matrix camera as well as the lens distortion of the laser triangulation sensor is corrected with the same algorithm, described in (Tardif et al., 2006), which is separated from the rest of the calibration. The used method belongs to the plumbline algorithms, which use the fact that straight lines remain straight under perspective transformations, and only takes account of the radial lens distortion.

Hence points of the calibration object, which are located in the real world on straight lines, are taken to determine the parameters of the lens distortion model. All data received from the cameras are rectified with this algorithm before they are used for further computations. Therefore we assume, in the algorithms presented below, that the lens distortion is already corrected. Hence we can use the pinhole camera model to describe the cameras of the sensor.

2.3 The Laser Triangulation Sensor

2.3.1 The Mathematical Model

At least for the calibration of the laser triangulation sensor, we require a linear relative motion between the sensor and the calibration object. Furthermore we assume that the absolute distances, which the calibration object is moved between two scanned profiles are unknown, but constant. Then the process of mapping a corner with the laser triangulation sensor from world coordinates C into pixel coordinates c can be described mathematically as follows.

First the position where the corner intersects the laser plane during a scan is computed. The coordinate C_{LP} of this point of intersection on the laser plane is received by projecting the corner along the direction of motion onto the laser plane:

$$C_{LP} = Pr_z \cdot LP^{-1} \cdot C \tag{1}$$

where

$$LP = \begin{pmatrix} v_1 & v_2 & d \end{pmatrix} \tag{2}$$

is a basis of $\mathbb{R}^3$, with v_1, v_2 are parallel to the laser plane, d represents the direction of motion of the profil scanner and

$$Pr_z = \begin{pmatrix} 1 & 0 & 0 \\ 0 & 1 & 0 \end{pmatrix} \tag{3}$$

is the projection matrix along the third coordinate. When the corner reaches the coordinates C_{LP} on the laser plane, it is illuminated by the laser and therefore seen by the camera of the sensor.

Since the camera only detects points which intersect the laser plane, its projection matrix is reduced to a invertible homography H^{-1}, which fulfills the following constraint:

$$\begin{pmatrix} c_x \\ c_z \\ 1 \end{pmatrix} \propto H^{-1} \cdot \begin{pmatrix} C_{LP} \\ 1 \end{pmatrix} \tag{4}$$

The last unknown pixel coordinate c_y of the corner can be computed by dividing the distance of the corner to the laser plane along the direction of motion through the distance v.

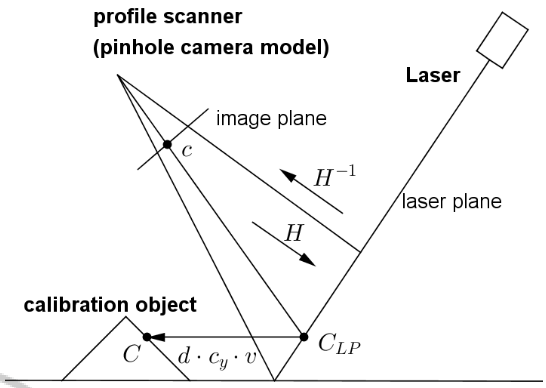

Figure 2: The mathematical model of the laser triangulation sensor.

According to this description of mapping the world coordinates of a corner of the calibration object onto its pixel coordinates, the used mathematical model consists of 14 degrees of freedom (DF):

v	...	distance between two profiles	1 DF
n	...	normal unit vector of the laser plane	2 DF
d_{LP}	...	the distance of the laser plane from the origin of the coordinate system	1 DF
d	...	direction of motion	2 DF
H	...	homography which maps points from the image onto the laser plane	8 DF

The aim of the calibration of the laser triangulation sensor is to determine the parameters, which are needed to transform the data provided by the sensor into the world coordinate system in which the calibration object is located.

2.3.2 Computing the Range Values of the Checkerboard Corners

While the scan number c_y and the x-coordinate on image plane c_x of the pixel coordinates c are received by applying a standard image processing algorithm for corner detection on the range image, we still have to determine the range value c_z.

For this reason we do not read out c_z, but fit a surface into the scanned checkerboard plane in a row-column-enviroment of c on the range image. The range value is then determined by the height of the corresponding surface at the corner coordinates c_x and c_y.

Besides of being more robust against noise, this method avoids two other problems, which occur dur-

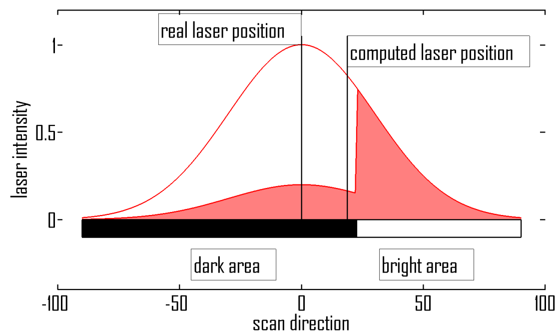

Figure 3: The laser line position above was determined by computing the center of gravity of the intensity of the reflected light. The missing reflections of the laser at the dark areas cause a wrong estimation of the laser line position.

ing the determination of the range values of the checkerboard corners:

1. If the corner is found on a black square of the checkerboard, there might be no range value received at its position, because the intensity of the reflected laser light was too low and the laserline could not be detected by the laser triangulation sensor.
2. All corners are located at bright/ dark transitions of the checkerboard pattern. At those locations the estimation of the laser stripe position (and consequently the corresponding range values) on the image plane gets biased, due to the change of the intensity of the reflected laser light. This situation is visualized in figure 3.

Since the surfaces are only used to locally describe the range image, the lens distortion has a negligible influence on the surface fit.

2.3.3 Computation of the Direction of Motion

The computation of the direction of motion d is based on the transformation of the world coordinates C of the corners into pixel coordinates c_x and c_z described in section 2.3.1. Since we are interested only in the determination of the direction of motion in this part of the calibration, we can simplify the problem by assuming that the laser plane is orthogonal to the direction of motion.
This rotation of the laserplane causes only a scaling of the coordinates C_{LP} of the projected corners in LP coordinates, followed by a scaling of the columnes of the homography H^{-1} with the result that the real world corner coordinates still are mapped onto their pixel counterparts. We also do not care about the orientation of v_1 and v_2 within the laser plane, because a transformation of these vectors can be undone in the same way with no effect on the computation of the direction of motion d.
For this reason we choose LP as an orthonormal basis, what makes the computation of its inverse easy.
As d should be a unit vector, it only depends on two angles α, β (spherical coordinates) and can be expressed as:

$$d = \begin{pmatrix} \cos(\alpha)\cos(\beta) \\ \cos(\alpha)\sin(\beta) \\ \sin(\alpha) \\ 0 \end{pmatrix} \tag{5}$$

$\Rightarrow$ Depending on d, v_1 and v_2 can be chosen:

$$v_1 = \begin{pmatrix} -\sin(\alpha)\cos(\beta) \\ -\sin(\alpha)\sin(\beta) \\ \cos(\alpha) \\ 0 \end{pmatrix}, \; v_2 = \begin{pmatrix} -\sin(\beta) \\ \cos(\beta) \\ 0 \\ 0 \end{pmatrix} \tag{6}$$

The process of mapping a corner from world coordinates can be condensed to one projective transformation T by using the projective counterparts $\widetilde{Pr_z}$ and $\widetilde{LP}^{-1}$ of Pr_z and LP^{-1}:

$$\begin{pmatrix} c_x \\ c_z \\ 1 \end{pmatrix} \propto \underbrace{H^{-1} \cdot \widetilde{Pr_z} \cdot \widetilde{LP}^{-1}}_{T} \cdot \begin{pmatrix} C \\ 1 \end{pmatrix} \tag{7}$$

The composed matrix T is determined with the help of the direct linear transformation algorithm.

As a consequence the computation of the vector, which represents the direction of motion, is reduced to the decomposition of the matrix T into the two factors H^{-1} and $\widetilde{Pr_z} \cdot \widetilde{LP}^{-1} =$

$$\begin{pmatrix} -\sin(\alpha)\cos(\beta) & -\sin(\alpha)\sin(\beta) & \cos(\alpha) & 0 \\ -\sin(\beta) & \cos(\beta) & 0 & 0 \\ 0 & 0 & 0 & 1 \end{pmatrix} \tag{8}$$

Calculating this decomposition yields the following result for the sperical coordinates of the direction of motion d:

$$\begin{aligned} \cos(\beta) &= \pm \sqrt{\frac{\begin{vmatrix} T_{1,2} & T_{1,3} \\ T_{2,2} & T_{2,3} \end{vmatrix}^2}{\begin{vmatrix} T_{1,2} & T_{1,3} \\ T_{2,2} & T_{2,3} \end{vmatrix}^2 + \begin{vmatrix} T_{1,1} & T_{1,3} \\ T_{2,1} & T_{2,3} \end{vmatrix}^2}} \\ \sin(\beta) &= \frac{\begin{vmatrix} T_{1,2} & T_{1,3} \\ T_{2,2} & T_{2,3} \end{vmatrix}}{\begin{vmatrix} T_{1,3} & T_{1,2} \\ T_{2,3} & T_{2,2} \end{vmatrix}} \cdot \cos(\beta) \\ \cos(\alpha) &= \pm \sqrt{\frac{T_{2,3}^2}{T_{2,3}^2 + \left(T_{2,2}\sin(\beta) + T_{2,1}\cos(\beta)\right)^2}} \\ \sin(\alpha) &= \frac{-\cos(\alpha)\left(T_{2,2}\sin(\beta) + T_{2,1}\cos(\beta)\right)}{T_{2,3}} \end{aligned} \tag{9}$$

- The computed vector d is only determined up to a multiplication with ± 1. The correct factor can be found by considering the order in which the corners of the checkerboard pattern intersected the laser plane.
- Permuting the rows on the left repectivly right side of equation 7 will cause a permutation of the rows respectively columns of matrix T. With this strategy the gimbal lock problem, which occurs at $\alpha = \pm\frac{\pi}{2}$, and numerical instabilities can be avoided.

2.3.4 Computation of the Laser Plane and the Distance between Two Profiles

The computation of the position of the laser plane is based on the known number of scanned profiles c_y, until a corners of the calibration object intersects the laser plane. Subtracting the vector $v \cdot c_y \cdot d$ from C yields a point, which is located on the laser plane (see figure 2) and therefore satisfies the following equation:

$$\langle C - vc_y d, n\rangle = d_{LP} \tag{10}$$

Since every corner of the calibration object must hold this equation, the unknown parameters v, d_{LP} and n are obtained by solving a non-linear optimization problem.

Using the normalized data $C_\mathrm{n} = \begin{pmatrix} C_1 & C_2 & C_3 \end{pmatrix}^\top$ respectively $c_{y\mathrm{n}}$, related to the coordinates C respectively c_y and by means of the method of Lagrange multipliers, a necessary condition for the normal unit vector n_n in form of the following eigenvalue problem is received (For reasons of simplicity there are no indices of summation in the equations, but summation always relate to the world and pixel coordinates of the corners $1 \dots N$):

$$\begin{aligned} A \cdot n_\mathrm{n} &= \lambda n_\mathrm{n} \\ \lambda &= \text{Lagrange multiplier} \\ A_{i,j} &= \textstyle\sum_{C_\mathrm{n}} C_i C_j - \frac{\sum_{C_\mathrm{n}} C_i c_{y\mathrm{n}} \sum_{C_\mathrm{n}} C_j c_{y\mathrm{n}}}{N} \end{aligned} \tag{11}$$

The unit eigenvector belonging to the smallest eigenvalue of matrix A is then the normal vector of the laser plane. Since scaling and shifting the corners has no influence on the orientation of the laser plane, n_n is also the normalvector of the laser plane related to the original corners coordinates C.

$$v_\mathrm{n} = \frac{\left\langle \sum_{C_\mathrm{n}} \left(C_\mathrm{n} c_{y\mathrm{n}}\right), n_\mathrm{n}\right\rangle}{N \langle n_\mathrm{n}, d\rangle} \tag{12}$$

$$d_{LP\mathrm{n}} = \frac{1}{N} \left\langle \textstyle\sum_{C_\mathrm{n}} \left(C_\mathrm{n} - v_\mathrm{n} c_{y\mathrm{n}} d\right), n_\mathrm{n}\right\rangle \tag{13}$$

Under taking into account the transformation between the coordinates C and C_n, the searched parameters v and d_{LP} can be obtained from v_n and $d_{LP\mathrm{n}}$.

2.3.5 Computation of the Homography

The last parameter to determine is the homography H, which maps points from the image plane of the laser triangulation camera onto the laser plane. On the one hand the coordinates, where the corners appeared on the image plane are $\begin{pmatrix} c_x & c_z \end{pmatrix}^\top$, on the other hand their projections on the laser plane $H \cdot \begin{pmatrix} c_x & c_z & 1 \end{pmatrix}^\top$ must coincide with the coordinates C_{LP} (see figure 2).
Since the direction of motion is already known and also a basis of the laser plane is obtained in the form of two eigenvectors of equation (11), the coordinates C_{LP} can be computed by means of equation (1).

The searched homography can then be determined according the following equation system:

$$\begin{pmatrix} C_{LP} \\ 1 \end{pmatrix} \propto H \cdot \begin{pmatrix} c_x \\ c_z \\ 1 \end{pmatrix} \tag{14}$$

This linear optimization problem can be solved by means of the direct linear transformation algorithm.

2.4 Calibration of the Color Camera

Because the lens distortion is corrected with a separated algorithm, as described in section 2.2, the pinhole camera model is used again to describe the color camera. Due to the 3D calibration object, the direct linear transformation algorithm can be used to determine the needed projection matrix. The advantage of this algorithm is that only one image of the calibration object is needed, which keeps the calibration process efficient.

In case of an installation of the 2D/3D sensor above a conveyor belt it is necessary to take the circumstance into account that the calibration object, and therefore also the world coordinate system, is moved during the calibration process.

However the color camera can be shifted to the correct position by taking advantage of the direction of motion vector d and the distance v, which are gained during the calibration of the laser triangulation sensor.

3 RESULTS

3.1 Combining the 3D Point Cloud with the Color Information

One possibility to evaluate the precision of the color mapping is to take advantage of the known positions of the calibration object corners. Starting in the range image, provided by the laser triangulation sensor, the pixel coordinates of the corners are transformed into world coordinates. The yielded reconstructed corner coordinates are then mapped, by means of the projection matrix of the color camera, onto the color image, which was used to calibrate the color camera. That projected corners should coincide with the corners of the checkerboards, which are shown in the image. The color mapping error then can be assessed by computing the Euclidean distance between the projected corners and the corners on the image, which are found by a corner detection algorithm.

Such an evalution is visualized on the figures 4 with a mean distance between the projected and found corners of 0.417 pixels and maximum and minimum distances amounting to 1.475 pixels and 0.012 pixels. However that evaluation also reflects the errors of the corner coordinate detection in the range image as well as in the color image.

3.1.1 An Example of a Colored Point Cloud

In this section we present an example of a colored point cloud. The scanned object was a multimeter, whose colored point cloud is visualised in figure 5.

4 CONCLUSIONS AND FUTURE WORK

The inovation of the presented 2D/3D vision sensor was the novel calibration of laser triangulation sensors, which does not treat the sensor as matrix camera with an additional laser, but as one composed sensor. All needed data are gained through one single scan of the calibration object and the subsequent computation of the sensor parameters is based on closed-form solutions.

A calibration object was proposed and it was described how to extract the corner coordinates from its scan.

The quality of mapping the color onto the 3D point cloud was examined in section 3.

However in the presented calibration the direct-linear-transformation algorithm is used, which minimizes an algebraic cost function instead of a geometric interpretable error. Furthermore the computation is done in three separated steps, whereby the calibration parameters are not optimized simultaneously what would be preferable.

For this reason it is planned to add another calibration step, which minimizes the reconstruction error of the corners and optimizes all calibration parameters simultaneously by means of a gradient methode.

The convergence of this algorithm can be ensured since the outcome of the calibration method presented above serves as starting guess for this iterative algorithm and the calibration parameters are only refined.

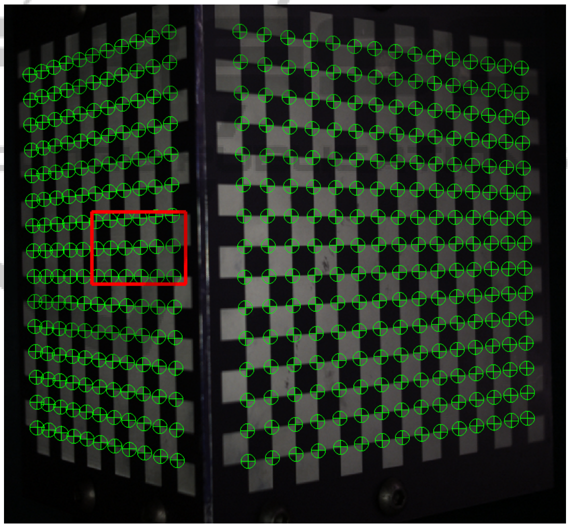

(a) The projections of the reconstructed corners of the calibration object.

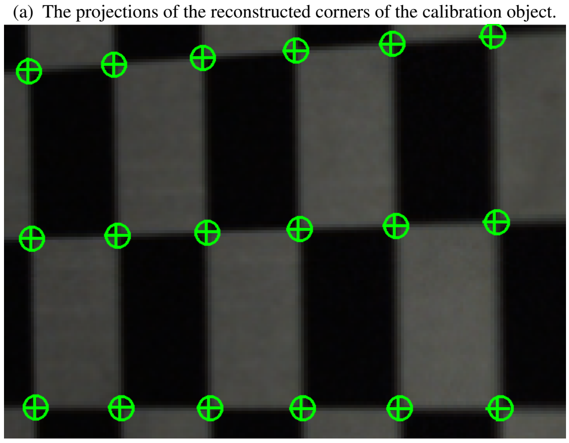

(b) An enlarged view of the region within the rectangular.

Figure 4: The circles on the image mark the corners, which are found with a corner detection algorithm. The projected 3D corners are visualized with the crosses.The projected corners do not perfectly coincide with the found corners marked by the circles.

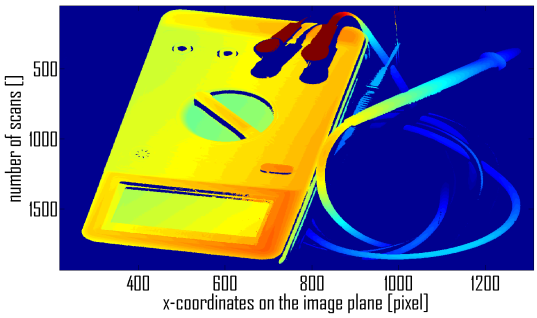

(a) The raw data provided from a laser triangulation sensor in form of a range image.

(b) The image of the color camera.

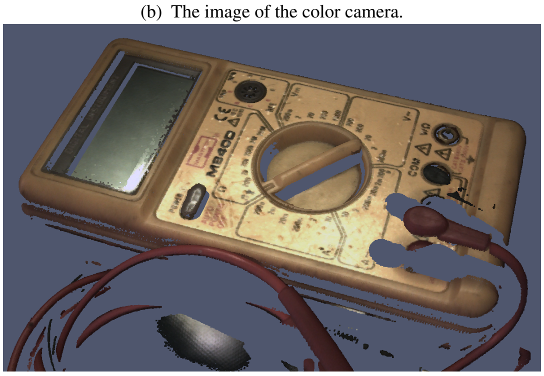

(c) The combined information in form of a 3D point cloud.

Figure 5: An example of a colored point cloud in form of a scanned multimeter.

ACKNOWLEDGEMENTS

The authors have been supported by the EC project FP7-ICT-270138 DARWIN.

The presented 2D/3D vision sensor was examined as a part of the DARWIN project. Moreover we want to thank our colleagues of the machine

REFERENCES

Abdel-Aziz, Y. and Karara, H. (1971). Direct linear transformation into object space coordinates in close-range photogrammetry. *In Proc. of the Symposium on Close-Range Photogrammetry*.

Bolles, R., Kremers, J., and Cain, R. (1981). A simple sensor to gather three-dimensional data. *Technical Report 249, SRI, Stanford University*.

McIvor, D. A. M. (2002). Calibration of a laser stripe profiler. *Optical Engineering 41*.

Munaro, M., Michieletto, S., So, E., Alberton, D., and Menegatti, E. (2011). Fast 2.5d model reconstruction of assembled parts with high occlusion for completeness inspection. *Fast 2.5D model reconstruction of assembled parts with high occlusion for completeness inspection*.

Tardif, J.-P., Sturm, P., and Roy, S. (2006). Self-calibration of a general radially symmetric distortion model. *In Proc. of the 9th European Conference on Computer Vision, Graz, Austria*.